Dynamic scaffold of chiral binaphthol derivatives with the alkynylplatinum(II) terpyridine moiety

Sammual Yu-Lut Leung, Wai Han Lam, and Vivian Wing-Wah Yam[1]

Institute of Molecular Functional Materials [Areas of Excellence Scheme, University Grants Committee (Hong Kong)] and Department of Chemistry, The University of Hong Kong, Hong Kong, People's Republic of China

This contribution is part of the special series of Inaugural Articles by members of the National Academy of Sciences elected in 2012.

Contributed by Vivian Wing-Wah Yam, January 24, 2013 (sent for review October 19, 2012)

Platinum(II)-containing complexes with inherently chiral binaphthol derivatives display a versatile scaffold between random coils and single-turn helical strands, in which the conformational transition is controlled by the Pt···Pt and π–π interactions of alkynylplatinum(II) terpyridine moiety upon solvent and temperature modulation. The bisignate Cotton effect in the circular dichroism spectra is indicative of the cooperative transformation from random coil state to a compact single-turn *M*- or *P*- helix. More importantly, as revealed by the appearance of new UV-vis absorption and emission bands during conformational change, the self-assembly of the platinum(II)-containing complex into a helical structure is assisted by the metal···metal and π–π interactions of the alkynylplatinum(II) terpyridine moieties. The folded structure with stabilization via metal···metal and π–π interactions has been supported by density functional theory calculations, which provide insights into the folded geometry of these kind of metallo-foldamers.

chirality | luminescence | noncovalent interactions | platinum complex

The photophysical and spectroscopic properties of the d^8 platinum(II) polypyridine system have been extensively studied (1–36) and are pioneered by the works of various groups, such as those of Miskowski and colleagues (1–3), Gray and colleagues (4–6), Lippard and colleagues (7–11), Che and colleagues (12–15), Vogler and colleagues (16), and McMillin and colleagues (17). Such square-planar platinum(II) complexes have been shown to exhibit interesting and intriguing photophysical properties associated with a tendency to form metal···metal and/or π–π stacking interactions (1–17). Most of the studies on these platinum(II) polypyridine systems related to the metal···metal interactions are mainly associated with their rich solid-state polymorphism and are confined to that in the study of solid-state spectroscopy and electronic structures (4, 8, 14). Corresponding studies in solution are relatively unexplored (8).

In view of the relatively small association constants for dimerization or oligomerization found for these compounds in solution, high solubility would be an important prerequisite for them in the preparation of solutions for the study of aggregation in solution. However, poor solubility of the platinum(II) polypyridine system is commonly encountered in solution and limits an extensive study of its aggregation properties in solution.

As an extension of our previous work on transition metal alkynyl complexes (37–45), efforts have been made to prepare the first luminescent alkynylplatinum(II) terpyridine system, $[Pt(tpy)(C{\equiv}CR)]^+$ (20), with improved solubility through the incorporation of strong σ-donating and solubilizing alkynyl ligands into the platinum(II) metal center. Apart from the rich photophysical and luminescence properties, as well as interesting solid-state polymorphism, such complexes exhibit notable color changes and luminescence enhancements as a result of Pt···Pt and π–π stacking interactions that occur from solvent composition change (21), polyelectrolyte addition (22, 23), and gel formation (24). Such studies have benefited from the early works on the understanding of the influence of the metal···metal interaction on the spectroscopic properties of the d^8 platinum(II) system (1–36, 46–54) and a recent study on the energy landscape of the ligand-bridged dinuclear iridium compound, which demonstrates the versatility of metal···metal interactions in governing the conformational change of the geometry (55). Apart from using metal···metal and π–π stacking interactions in stabilizing supramolecular nanostructures (28), hairpin conformation (25), and organogel formation (24), our group recently demonstrated the utilization of Pt···Pt and π–π interactions in controlling the helix-coil transition in *meta*-phenylene ethynylene (*m*PE) oligomers and in stabilizing reversibly the construction of a single-turn helix (26). The use of metallophilic interactions as the driving force has opened up a new strategy for the construction of helical strands of metallo-foldamers that are of immense interest in supramolecular architectures.

Chiral supramolecular chemistry has also been of great interest over the last decade, with its profound potential for enantioselective applications (56–80), such as chiral separation (64, 65), molecular discrimination (66–69), asymmetric synthesis (70–72), liquid crystals (73–75), nonlinear optics (76, 77), and so forth. One representative class of chiral moiety is the 1,1-binaphthyls, which have extensive applications in molecular recognition (81–84), asymmetric catalysis (85), and materials (86). There are numerous examples of using 1,1-binaphthyl derivatives to achieve polygons (87) or helicates (88, 89), in which the conformational preference is limited due to a strong metal–ligand coordination. In contrast, interest in foldamers with versatile scaffolds has increased significantly because of their well-defined yet dynamic conformations that can be highly responsive to external stimuli (90–93). The introduction of inherently chiral binaphthol segments to construct a foldamer is very rare (90, 93). These examples use π–π stacking interactions (90) and hydrogen bonding (93) to transform the scaffold of binaphthol into helical strands in solution. Therefore, in contrast to those binaphthol-based helicates with irreversible conformational change using strong metal–ligand coordination, we herein report a series of metallo-foldamers using metal···metal interactions to control structural changes from random coil to helical strand upon solvent and temperature modulation. The present study demonstrates the ability of noncovalent metal···metal interactions in assisting the conformational change of a binaphthol-based complex in a metallo-foldamer system, with the modulation of electronic absorption, emission, and circular dichroism spectroscopic properties.

Results and Discussion

Our design is based on the incorporation of alkynylplatinum(II) terpyridine units into the single-turn backbone of a binaphthol derivative. The preparation of the binaphthol derivatives involves

Author contributions: V.W.-W.Y. designed research; S.Y.-L.L. and W.H.L. performed research; and S.Y.-L.L., W.H.L., and V.W.-W.Y. wrote the paper.

The authors declare no conflict of interest.

See Profile on page 7964.

[1]To whom correspondence should be addressed. E-mail: wwyam@hku.hk.

This article contains supporting information online at www.pnas.org/lookup/suppl/doi:10.1073/pnas.1301252110/-/DCSupplemental.

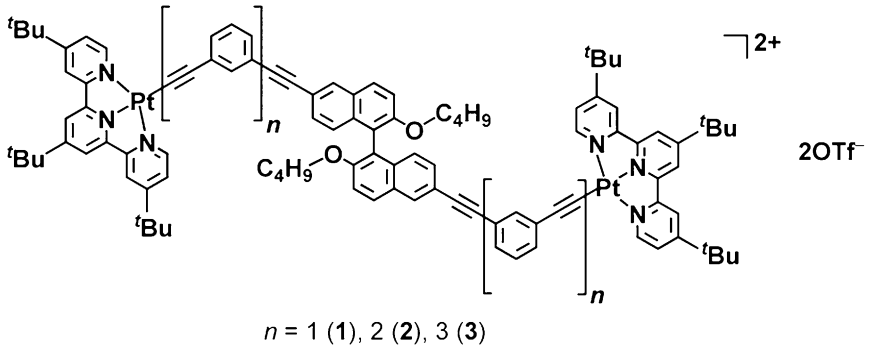

n = 1 (**1**), 2 (**2**), 3 (**3**)

Fig. 1. Structures of complexes **1**–**3**.

first the alkylation of 6,6′-dibromo-1,1′-bi-2-naphthol with ^{n}BuBr, followed by the palladium-catalyzed coupling reaction with the corresponding *m*PE repeating units, H-(C≡C-1,3-C_6H_4)$_n$-C≡C-Si^{i}Pr$_3$ (*n* = 1, 2, and 3), to afford the bis-coupled products. The detailed synthetic route is given in Scheme S1. Complexes **1**–**3** as shown in Fig. 1 were synthesized by reacting the corresponding binaphthol derivatives with [(^{t}Bu$_3$tpy)PtCl](OTf) in a molar ratio of 1:2 in degassed dimethylformamide (DMF) containing NEt_3 with a catalytic amount of CuI. The enantiomers in the (*S*)-form were prepared for all of the complexes for comparison, whereas only **2** was synthesized in both enantiomeric forms. All of the complexes have been characterized by ^{1}H and ^{13}C NMR, IR spectroscopy, fast atom bombardment (FAB) mass spectrometry, and elemental analyses.

Complex **1** gives a pale yellow solution in CH_2Cl_2, and the electronic absorption spectrum shows intense intraligand (IL) [π→π*] transitions of the terpyridine and alkynyl ligands at about 303–330 nm, together with low-energy absorptions at 430–470 nm, which are assigned as metal-to-ligand charge transfer (MLCT) [dπ(Pt)→π*(tpy)] transitions mixed with alkynyl-to-terpyridine ligand-to-ligand charge transfer (LLCT) [π(C≡CR)→π*(tpy)] character. When the solvent is changed from CH_2Cl_2 to CH_3CN, a negative solvatochromism of the MLCT absorption band (26) is observed, with a blue shift to 408–441 nm (Fig. S1*A*). The circular dichroism (CD) spectra of (*S*)-**1** in CH_2Cl_2 and CH_3CN also show similar behavior (Fig. S1*B*), indicating that the ellipticity originates from the chromophore of the inherently chiral binaphthol backbone in both CH_2Cl_2 and CH_3CN (90). In sharp contrast to the observation of **1**, complex **2**, which is bis-coupled with two *m*PE units on the backbone (*n* = 2), shows a significant decrease in the intraligand [π→π*(C≡CR)] absorption band at 278–340 nm, indicative of a conformational change of the binaphthol backbone from the *transoid* to the *cisoid* form upon increasing the CH_3CN content in CH_2Cl_2, and the emergence of a low-energy absorption tail at 510 nm starting from 40% CH_3CN onward (Fig. S2). With reference to our previous works (21–27), the appearance of the absorption tail at longer wavelengths is ascribed to the formation of metal···metal interactions, and the absorption tail is tentatively assigned as the metal-metal-to-ligand charge transfer (MMLCT) transition. Because the absorption tail at 510 nm in CH_3CN is found to obey Beer's law within the concentration range of 10^{-6}–10^{-4} M, it establishes the MMLCT transition as being one that is of an intramolecular association in nature. Concomitant with the change in the UV-vis absorption spectra, (*S*)-**2** demonstrates a remarkable Cotton effect, with the growth of a new band at 307 nm and a diminution of the band at 290 nm in the CD spectra upon increasing the CH_3CN content in CH_2Cl_2 (Fig. 2, *Upper*). This bisignate Cotton effect in the CD spectra at high CH_3CN contents arises from the alteration of the chiral environment for the helical backbone resulting in the twist sense bias of the helix, indicative of the formation of a single-turn *P*-helix, which could not have been observed in the pure organic counterpart for such a short chain with sole π–π stacking interactions (90). Furthermore, the planarization of the terpyridine moieties brought about by coordination to the Pt(II) metal center would facilitate the formation of the single-turn metallohelix via Pt···Pt and π–π stacking interactions, which is distinct from those classically observed in the pure organic counterpart with sole π–π stacking interactions.

Moreover, it is important to note the presence of isodichroic points at 279 and 300 nm, which shows that this conformational change involves a two-state equilibrium (90). The CD spectra of (*R*)-**2** show a similar trend, except that the CD signals are mirror images of that for (*S*)-**2**, resulting from the formation of the *M*-helix as shown in Fig. 2 (*Lower*). Therefore, it is plausible that **2** would undergo a solvophobically driven process from the random coil state to the helical strand. Such helical bias is due to the self-assembly of two platinum(II) terpyridine moieties resulting from the intramolecular metal···metal and π–π interactions at high CH_3CN contents. By monitoring the changes of A_{341nm}/A_{290nm} in the UV-vis spectra and the ellipticity at 307 nm in the CD spectra, sigmoidal curves typical of cooperative interactions are observed (Fig. 3), with helix stabilization energies $\Delta G(CH_3CN)$ of −1.71 ± 0.02 and −1.80 ± 0.02 kcal/mol obtained (Table 1) from the two independent experiments, which are in close agreement with each other.

Density functional theory (DFT) calculations were performed to provide insight into the molecular structure of the folded conformation in (*S*)-**2** (see the Computational Details). As shown in Fig. 4, the binaphthol backbone containing the couple of two *m*PE units

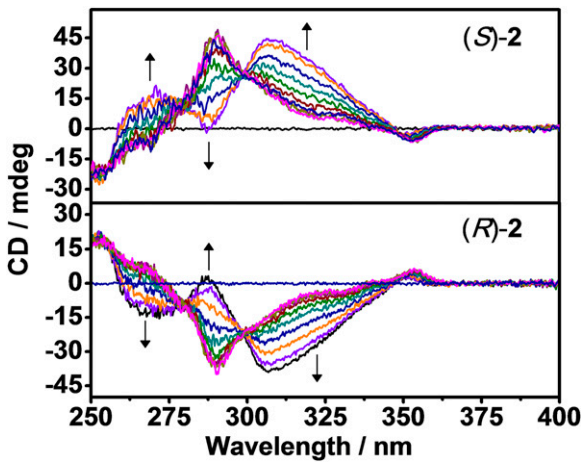

Fig. 2. CD spectral traces of (*S*)-**2** (2.4 × 10^{-5} M) (*Upper*) and (*R*)-**2** (2.3 × 10^{-5} M) (*Lower*) in CH_2Cl_2 with increasing CH_3CN content in CH_2Cl_2 at 298 K.

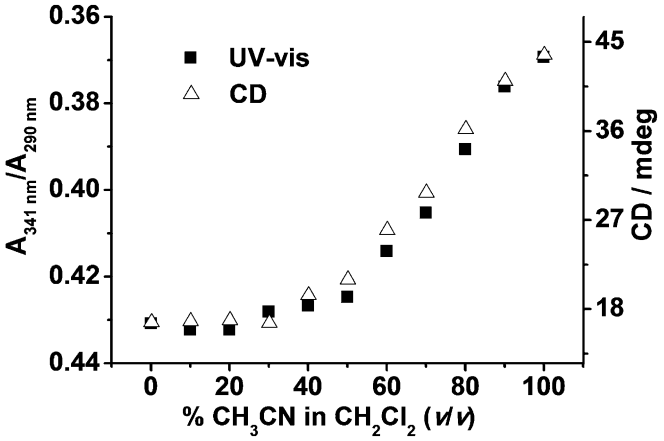

Fig. 3. Solvent denaturation of **2** measured by UV-vis absorbance ratios of $A_{341\ nm}/A_{290\ nm}$ (■) and CD intensity at 307 nm (△).

($n = 2$) forms a single turn of the *P*-helix. The two [(^{t}Bu$_3$tpy)Pt] units are located outside the helical turn, with the two terpyridyl groups arranged in a staggered conformation. The Pt···Pt distance and interplanar distance of the two [Pt(^{t}Bu$_3$tpy)] coordination planes are calculated to be 3.349 and 3.451 Å, respectively, indicating the presence of Pt···Pt and π–π interactions in the folded structure. The change in the free energy of the folded structure with respect to the unfolded structure (all-*transoid* conformation in the *m*PE and binaphthol backbone) as shown in Fig. S3 was computed to be −1.9 kcal/mol,* which is close to the experimental value and further supportive of the stabilization of the folded structure by metal···metal and π–π interactions.

By analogy to **2**, complex **3** bis-coupled with three *m*PE units ($n = 3$) also shows the behavior of folding with the formation of metal···metal and π–π interactions upon increasing the CH_3CN content in CH_2Cl_2, as revealed from the UV-vis and CD spectra shown in Fig. S4 *A* and *B*, respectively. The helix stabilization energy was found to be less negative, with $\Delta G(CH_3CN)$ values of -0.86 ± 0.05 and -0.84 ± 0.04 kcal/mol obtained from UV-vis and CD experiments, respectively. The misalignment of the two terminal platinum(II) terpyridine units in the single turn probably accounts for the less stable helical strand with less favorable ΔG values when $n = 3$.

*We have computed 10 possible unfolded structures with various possible arrangements of the *cis* or *trans* configuration of the *m*PE and binaphthol backbone. The change in the free energy of the unfolded structures with respect to the folded structure is all positive, indicating the folded structure is the most stable. Several of them give a similar change in the free energy as the all-*transoid* structure shown in Fig. S3.

Table 1. Helix stabilization energy in pure CH_3CN [$\Delta G(CH_3CN)$] for 2 and 3 obtained from the titration curves in UV-vis and CD spectra

	$\Delta G(CH_3CN)$/kcal mol^{-1}	
Complex	UV	CD
2	−1.71	−1.80
3	−0.86	−0.84

The importance of the platinum(II) terpyridine moiety in governing the conformational transition is most apparent in variable temperature UV-vis absorption and CD measurements in CH_3CN. Upon increasing the temperature from 293 to 353 K in CH_3CN, the UV-vis spectra of **2** show a disappearance of the MMLCT absorption band (Fig. S5), whereas in the CD spectra, a diminution of ellipticity at 307 nm for (*S*)- and (*R*)-**2** was observed, as shown in Fig. S6 *A* and *B*, respectively. The spectral changes in the UV-vis and CD spectroscopy clearly indicate that, upon increasing the temperature, the helical bias of the helix would significantly decrease due to the destruction of the metal···metal and π–π interactions of the alkynylplatinum(II) terpyridine moiety, leading to the transformation from the folded state back to the random coil state. Therefore, it is believed that the platinum(II) terpyridine moiety plays an important role in governing the dynamic scaffold of the binaphthol derivatives between the random coil and the helical strand upon modulations by various stimuli, as depicted schematically in Fig. 5.

Complexes **1**–**3** exhibit strong emission bands in CH_2Cl_2 at 577–582 nm upon excitation at $\lambda > 400$ nm, which are assigned as an excited state of predominantly ^{3}MLCT/^{3}LLCT character. Upon increasing the CH_3CN content, **2** and **3** both show a growth of a low-energy emission band at 685 nm typical of a ^{3}MMLCT emission with the diminution of the ^{3}MLCT/^{3}LLCT emission of the monomeric alkynylplatinum(II) terpyridine moiety (Fig. 6 *A* and *B*). Interestingly, **2** with the optimum length for a single-turn helical strand shows a switching-off of the monomeric ^{3}MLCT/^{3}LLCT emission and a more red-shifted ^{3}MMLCT emission band in CH_3CN (Fig. S7*A*), in accordance with the proposition that **2** would form a more stable helical strand with a tighter conformation than **3**, as reflected by the more negative $\Delta G(CH_3CN)$ value of **2** than **3**. In contrast, the emission maximum of **1** in CH_3CN only shows a slight blue shift

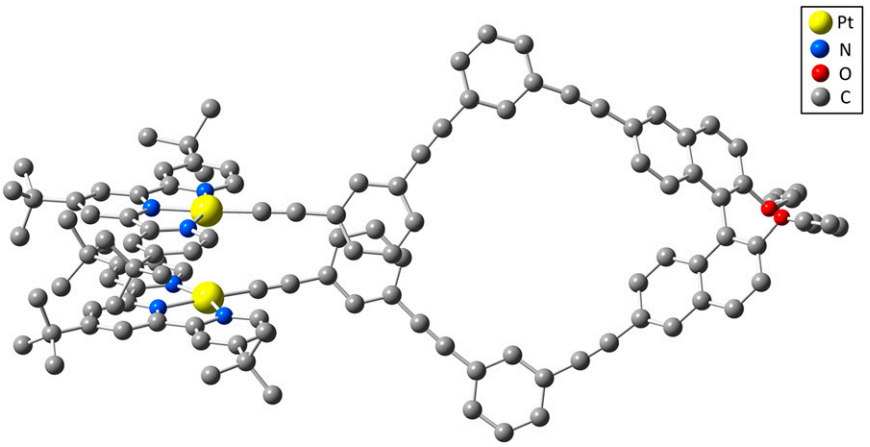

Fig. 4. Optimized structure of the helical conformation in (*S*)-**2**.The hydrogen atoms are omitted for clarity.

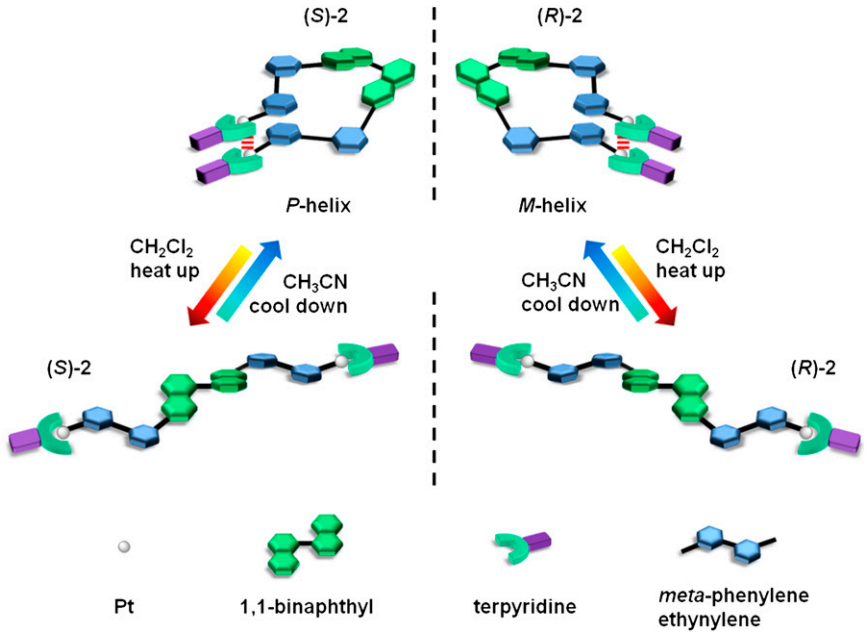

Fig. 5. Schematic representation of the dynamic transformation of binaphthol derivatives between random coils and single-turn helical strands by temperature and solvent modulation.

relative to that observed in CH_2Cl_2 (Fig. S7*B*) due to the negative solvatochromism (35), without the self-assembly of the two platinum(II) terpyridine moieties to form metal···metal and π–π interactions. In the variable temperature luminescence study, upon increasing the temperature, both **2** and **3** show a decrease in ^{3}MMLCT emission as shown in Fig. S7 *C* and *D*, respectively, indicating that these metallo-foldamers possess a high reversibility for the transformation from a helical strand back to a random coil with the reversible control of the metal···metal interactions for the folding process.

Summary and Prospects

In conclusion, we demonstrated a unique class of metallo-foldamers using inherently chiral binaphthol segments to construct a single-turn helical strand. Moreover, these metal-containing binaphthol derivatives display a structural conformational transition between the random coil state and the helical strand induced by different stimuli with the modulation of metal···metal and π–π interactions. The present work demonstrates the versatility and the reversibility of the metal···metal and π–π interactions in the stabilization of dynamic metallo-foldamers in diverse structural architectures that are distinct from those classically observed with metal–ligand coordination. The solvophobically tubular cavity of the helix with the inherently chiral binaphthol segment may be effective for molecular recognition and molecular switching by monitoring the loss of stereochemical information.

Materials and Methods

General Details. ^{1}H NMR spectra were recorded on a Bruker AVANCE 400 or 500 (400 and 500 MHz) Fourier-transform NMR spectrometer with chemical shifts reported relative to tetramethylsilane, $[(CH_3)_4Si]$. Positive-ion FAB mass spectra were recorded on a Thermo Scientific DFS high-resolution magnetic sector mass spectrometer. IR spectra were obtained as a KBr disk on a Bio-Rad FTS-7 Fourier transform infrared spectrophotometer (4,000–400 cm^{-1}). Elemental analyses of the complexes were performed on a Flash EA 1112 elemental analyzer at the Institute of Chemistry, Chinese Academy of Sciences. The UV-visible spectra were obtained using a Hewlett-Packard 8452A diode array spectrophotometer. The emission spectra at room temperature were recorded on a Spex Fluorolog-3 model FL3-211 fluorescence spectrofluorometer equipped with an R2658P PMT detector. Variable temperature UV-vis absorption and emission spectra were obtained using a Varian Cary 50 UV-vis spectrophotometer and a Spex Fluorolog-3 model FL3-211 fluorescence spectrofluorometer equipped with an R2658P PMT detector, respectively. The temperature was maintained by a Varian Cary single-cell Peltier thermostat.

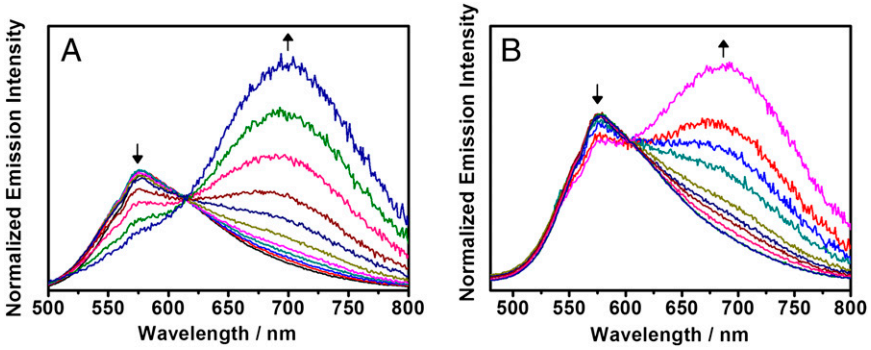

Fig. 6. Normalized emission spectral traces of CH_3CN-CH_2Cl_2 mixtures: 0–100% for (*A*) *rac*-**2** (2.4×10^{-5} M) at 616 nm with $\lambda_{exc} = 435$ nm and (*B*) *rac*-**3** (2.0×10^{-5} M) at 606 nm with $\lambda_{exc} = 420$ nm upon increasing the CH_3CN fraction.

Synthetic Details. The synthesis of the binaphthol derivatives involves the alkylation of 6,6′-dibromo-1,1′-bi-2-naphthol with ^{n}BuBr, followed by the Sonogashira coupling reactions with the corresponding *m*PE repeating units [H-(C≡C-1,3-C_6H_4)$_n$-C≡C-Si^{i}Pr$_3$ (n = 1, 2, and 3)], to afford the bis-coupled products. After removing the triisopropylsilyl (TIPS) protecting groups with tetra-*n*-butylammonium fluoride, the terminal alkynes of various lengths were synthesized. Complexes **1**–**3** were synthesized by reacting the corresponding binaphthol alkyne derivatives with [(^{t}Bu$_3$tpy)PtCl](OTf) in a molar ratio of 1:2 in degassed DMF containing NEt_3 with a catalytic amount of CuI. The details of the synthesis and characterization are given in *SI Synthesis and Characterization* and Scheme S1.

Computational Details. Calculations were carried out using the Gaussian 09 software package (94). The folded and unfolded structures for (*S*)-**2** were fully optimized in solution (CH_3CN) using the density functional theory at the M06 level of theory (95) in conjunction with the solvation model density (SMD) continuum method (96). The Cartesian coordinate of the selected structures is shown in Table S1. The M06 functional has been recommended for the study of the noncovalent interactions and transition metal thermochemistry (97). The Stuttgart effective core potentials (ECPs) and the associated basis set were applied to describe Pt (98) with two f-type polarization functions (ζ = 0.70 and 1.14) (99), whereas the 6–31G(d) basis set (100–102) was used to describe all other atoms. Vibrational frequencies were calculated at the same level of theory for the optimized structures to verify that each was a minimum on the potential surface. Single point calculations were performed on the optimized structures using a larger basis set, in which the same metal basis set was used, but Dunning's correlation-consistent cc-pVTZ basis set (103) was used for all other atoms. The Gibbs free energies were computed at the M06/SMD(CH_3CN)/cc-pVTZ//M06/SMD(CH_3CN)/6–31g(d) level, in which thermal contributions to the free energy were obtained from the vibrational frequency calculations with the smaller basis set. A pruned (99,590) grid was used for all of the DFT calculations.

ACKNOWLEDGMENTS. Dr. A.Y.-Y. Tam is acknowledged for helpful discussions. We thank the Computer Center of The University of Hong Kong for providing computational resources. V.W.-W.Y. acknowledges the support from the University Research Committee (URC) Strategic Research Theme on Molecular Materials. This work was supported by the University Grants Committee Areas of Excellence (AoE) Scheme (AoE/P-03/08) and a General Research Fund (GRF) grant from the Research Grants Council of Hong Kong Special Administrative Region, P. R. China (HKU 7064/11P). S.Y.-L.L. acknowledges the receipt of a Hung Hing Ying Scholarship and a postgraduate studentship, both administered by The University of Hong Kong.

1. Miskowski VM, Houlding VH (1989) Electronic spectra and photophysics of platinum (II) complexes with α-diimine ligands. solid-state effects. 1. Monomers and ligand π dimers. *Inorg Chem* 28(8):1529–1533.
2. Houlding VH, Miskowski VM (1991) The effect of linear chain structure on the electronic structure of platinum(II) diimine complexes. *Coord Chem Rev* 111:145–152.
3. Miskowski VM, Houlding VH (1991) Electronic spectra and photophysics of platinum (II) complexes with α-diimine ligands solid-state effects. 2. Metal-metal interaction in double salts and linear chains. *Inorg Chem* 30(23):4446–4452.
4. Bailey JA, et al. (1995) Electronic spectroscopy of chloro-(terpyridine)platinum(II). *Inorg Chem* 34(18):4591–4599.
5. Hill MG, Bailey JA, Miskowski VM, Gray HB (1996) Spectroelectrochemistry and dimerization equilibria of chloro-(terpyridine)platinum(II). Nature of the reduced complexes. *Inorg Chem* 35(16):4585–4590.
6. Connick WB, Marsh RE, Schaefer WP, Gray HB (1997) Linear-chain structures of platinum(II) diimine complexes. *Inorg Chem* 36(5):913–922.
7. Jennette KW, Gill JT, Sadownick JA, Lippard SJ (1976) Metallointercalation reagents. Synthesis, characterization, and structural properties of thiolato(2,2′,2″-terpyridine) platinum(II) complexes. *J Am Chem Soc* 98(20):6159–6168.
8. Lippard SJ (1978) Platinum complexes: Probes of polynucleotide structure and antitumor drugs. *Acc Chem Res* 11(5):211–217.
9. Barton JK, Lippard SJ (1979) Cooperative binding of a platinum metallointercalation reagent to poly(A).poly(U). *Biochemistry* 18(12):2661–2668.
10. Hollis LS, Lippard SJ (1983) Synthesis, structure, and platinum-195 NMR studies of binuclear complexes of *cis*-diammineplatinum(II) with bridging α-pyridonate ligands. *J Am Chem Soc* 105(11):3494–3503.
11. O'Halloran TV, Roberts MM, Lippard SJ (1984) Correlation between metal-metal distances and optical spectroscopy in the platinum blues: Synthesis, crystal structure, and electronic spectrum of ethylenediamine platinum α-pyridone blue. *J Am Chem Soc* 106(21):6427–6428.
12. Che C-M, Wan KT, He LY, Poon C-K, Yam VW-W (1989) Novel luminescent platinum (II) complexes – photophysics and photochemistry of Pt(5,5′-dimethyl-2,2′-bipyridine)$(CN)_2$. *J Chem Soc Chem Commun* 14:943–944.
13. Che C-M, He L-Y, Poon C-K, Mak TCW (1989) Solid-state emission of dicyanoplatinum (II) and -palladium(II) complexes of substituted 2,2′-bipyridines and 1,10-phenanthroline and x-ray crystal structures of isomorphous M(bpy)(CN), (bpy = 2,2′-Bipyridine; M = Pt, Pd). *Inorg Chem* 28(15):3081–3083.
14. Yip HK, Cheng LK, Cheung KK, Che C-M (1993) Luminescent platinum(II) complexes. Electronic spectroscopy of platinum(II) complexes of 2,2′:6′,″-terpyridine (terpy) and *p*-substituted phenylterpyridines and crystal structure of. *J Chem Soc Dalton Trans* 22(19):2933–2938.
15. Lu W, Chui SS-Y, Ng K-M, Che C-M (2008) A submicrometer wire-to-wheel metamorphism of hybrid tridentate cyclometalated platinum(II) complexes. *Angew Chem Int Ed Engl* 47(24):4568–4572.
16. Kunkely H, Vogler A (1990) Photoluminescence of [Pt^{II}(4,7-diphenyl-1,10-phenanthroline)$(CN)_2$] in solution. *J Am Chem Soc* 112(14):5625–5627.
17. Aldrige TK, Stacy EM, McMillin DR (1994) Studies of the room-temperature absorption and emission spectra of $[Pt(trpy)X]^+$ systems. *Inorg Chem* 33(4):722–727.
18. Bevilacqua JM, Eisenberg R (1994) Quenching studies of the excited state of (4,7-Diphenylphenanthroline)(1-(ethoxycarbony1)-1-cyano- ethylene-2,2-dithiolato)platinum(II), Pt(Ph_2phen)(ecda), by aromatic amines and metallocenes and determination of its excited-state reduction potential. *Inorg Chem* 33(9):1886–1890.
19. Chan C-W, Cheng L-K, Che C-M (1994) Luminescent donor-acceptor platinum(II) complexes. *Coord Chem Rev* 132:87–97.
20. Yam VW-W, Tang RP-L, Wong KM-C, Cheung K-K (2001) Synthesis, luminescence, electrochemistry, and ion-binding studies of platinum(II) terpyridyl acetylide complexes. *Organometallics* 20(22):4476–4482.
21. Yam VW-W, Wong KM-C, Zhu N (2002) Solvent-induced aggregation through metal...metal/π...π interactions: Large solvatochromism of luminescent organoplatinum(II) terpyridyl complexes. *J Am Chem Soc* 124(23):6506–6507.
22. Yu C, Wong KM-C, Chan KH-Y, Yam VW-W (2005) Polymer-induced self-assembly of alkynylplatinum(II) terpyridyl complexes by metal...metal/π...π interactions. *Angew Chem Int Ed Engl* 44(5):791–794.
23. Yu C, Chan KH-Y, Wong KM-C, Yam VW-W (2006) Single-stranded nucleic acid-induced helical self-assembly of alkynylplatinum(II) terpyridyl complexes. *Proc Natl Acad Sci USA* 103(52):19652–19657.
24. Tam AY-Y, Wong KM-C, Wang G, Yam VW-W (2007) Luminescent metallogels of platinum(II) terpyridyl complexes: Interplay of metal...metal, π-π and hydrophobic-hydrophobic interactions on gel formation. *Chem Commun (Camb)* 20:2028–2030.
25. Yam VW-W, Chan KH-Y, Wong KM-C, Chu BW-K (2006) Luminescent dinuclear platinum(II) terpyridine complexes with a flexible bridge and "sticky ends" *Angew Chem Int Ed Engl* 45(37):6169–6173.
26. Leung SY-L, Tam AY-Y, Tao C-H, Chow HS, Yam VW-W (2012) Single-turn helix-coil strands stabilized by metal···metal and π-π interactions of the alkynylplatinum(II) terpyridyl moieties in *meta*-phenylene ethynylene foldamers. *J Am Chem Soc* 134(2): 1047–1056.
27. Wong KM-C, Yam VW-W (2011) Self-assembly of luminescent alkynylplatinum(II) terpyridyl complexes: Modulation of photophysical properties through aggregation behavior. *Acc Chem Res* 44(6):424–434.
28. Po C, Tam AY-Y, Wong KM-C, Yam VW-W (2011) Supramolecular self-assembly of amphiphilic anionic platinum(II) complexes: A correlation between spectroscopic and morphological properties. *J Am Chem Soc* 133(31):12136–12143.
29. Lu W, et al. (2003) Structural basis for vapoluminescent organoplatinum materials derived from noncovalent interactions as recognition components. *Chemistry* 9(24): 6155–6166.
30. Lu W, et al. (2004) Light-emitting tridentate cyclometalated platinum(II) complexes containing σ-alkynyl auxiliaries: Tuning of photo- and electrophosphorescence. *J Am Chem Soc* 126(15):4958–4971.
31. McGarrah JE, Kim Y-J, Hissler M, Eisenberg R (2001) Toward a molecular photochemical device: A triad for photoinduced charge separation based on a platinum diimine bis(acetylide) chromophore. *Inorg Chem* 40(18):4510–4511.
32. Wadas TJ, Lachicotte RJ, Eisenberg R (2003) Synthesis and characterization of platinum diimine bis(acetylide) complexes containing easily derivatizable aryl acetylide ligands. *Inorg Chem* 42(12):3772–3778.
33. Chakraborty S, et al. (2005) Synthesis, structure, characterization, and photophysical studies of a new platinum terpyridyl-based triad with covalently linked donor and acceptor groups. *Inorg Chem* 44(18):6284–6293.
34. Jarosz P, et al. (2009) Platinum(II) terpyridyl-acetylide dyads and triads with nitrophenyl acceptors via a convenient synthesis of a boronated phenylterpyridine. *Inorg Chem* 48(6):2420–2428.
35. Yang Q-Z, Wu L-Z, Wu Z-X, Zhang L-P, Tung C-H (2002) Long-lived emission from platinum(II) terpyridyl acetylide complexes. *Inorg Chem* 41(22):5653–5655.
36. Whittle CE, Weinstein JA, George MW, Schanze KS (2001) Photophysics of diimine platinum(II) bis-acetylide complexes. *Inorg Chem* 40(16):4053–4062.
37. Yam VW-W, Lau VC-Y, Cheung K-K (1996) Synthesis and photophysics of luminescent rhenium(I) acetylides-precursors for organometallic rigid-rod materials. X-ray crystal structures of [Re(^{t}Bu$_2$bpy)$(CO)_3$(^{t}BuC≡C)] and [Re(^{t}Bu$_2$bpy)$(CO)_3$Cl]. *Organometallics* 14(6):2749–2753.
38. Yam VW-W, Lau VC-Y, Cheung K-K (1996) Luminescent rhenium(I) carbon wires: Synthesis, photophysics, and electrochemistry. X-ray crystal structure of [Re(^{t}Bu$_2$bpy)$(CO)_3$(C≡CC≡C)Re(^{t}Bu$_2$bpy)$(CO)_3$]. *Organometallics* 15(6):1740–1744.
39. Yam VW-W, Choi SW-K (1996) Synthesis, photophysics and photochemistry of alkynylgold(I) phosphine complexes. *J Chem Soc Dalton Trans* 25(22):4227–4232.
40. Yam VW-W, Fung WK-M, Cheung K-K (1996) Synthesis, structure, photophysics, and excited-state redox properties of the novel luminescent tetranuclear

acetylidocopper(I) complex $[Cu_4(\mu\text{-dppm})_4(\mu_4\text{-}\eta^1,\eta^2\text{-}C{\equiv}C\text{-})](BF_4)_2$. *Angew Chem Int Ed Engl* 35(10):1100–1102.
41. Yam VW-W, Fung WK-M, Cheung K-K (1997) Synthesis, photophysics and crystal structures of hexanuclear copper(I) and silver(I) acetylide complexes. *Chem Commun* 10:963–964.
42. Yam VW-W, Fung WK-M, Wong M-T (1997) Synthesis, photophysics, electrochemistry, and excited-state redox properties of trinuclear copper(I) acetylides with bis (diphenylphosphino)alkylamines and -arylamines as bridging ligands. *Organometallics* 16(8):1772–1778.
43. Yam VW-W, Lo KK-W, Wong KM-C (1999) Luminescent polynuclear metal acetylides. *J Organomet Chem* 578(1-2):3–30.
44. Yam VW-W (2001) Luminescent carbon-rich rhenium(I) complexes. *Chem Commun* 14:789–796.
45. Yam VW-W (2002) Molecular design of transition metal alkynyl complexes as building blocks for luminescent metal-based materials: Structural and photophysical aspects. *Acc Chem Res* 35(7):555–563.
46. Roundhill DM, Gray HB, Che C-M (1989) Pyrophosphito-bridged diplatinum chemistry. *Acc Chem Res* 22(2):55–61.
47. Yersin H, Gliemann G (1985) Spectroscopic properties of the quasi-one-dimensional tetracyanoplatinate(II) compounds. *Struct Bonding* 62:87–153.
48. Gliemann G (1986) Magnetic field effects on the luminescence of transition metal complexes. *Comments Inorg Chem* 5:263–284.
49. Biedermann J, Gliemann G, Klement U, Range K-J, Zabelt M (1990) Spectroscopic studies of cyclometalated platinum(II) complexes: Superposition of two different spectroscopic species in the electronic spectra of a single crystal of $[Pt(bpm)(CN)_2]$ (bpm = 2,2′-Bipyrimidine). *Inorg Chem* 29(10):1884–1888.
50. Yersin H, Donges D (2001) Low-lying electronic states and photophysical properties of organometallic Pd(II) and Pt(II) compounds. Modern research trends presented in detailed case studies. *Top Curr Chem* 214:81–186.
51. Chassot L, Von Zelewsky A, Sandrini D, Maestri M, Balzani V (1986) Photochemical preparation of luminescent platinum(IV) complexes via oxidative addition on luminescent platinum(II) complexes. *J Am Chem Soc* 108(19):6084–6085.
52. Sandrini D, Maestri M, Balzani V, Chassot L, von Zelewsky A (1987) Photochemistry of the orthometalated *cis*-bis[2-(2-thienyl)pyridine]- platinum(II) complex in halocarbon solvents. *J Am Chem Soc* 109(25):7720–7724.
53. Che C-M, Yam VW-W, Wong W-T, Lai T-F (1989) Spectroscopy and x-ray crystal structure of luminescent $Pt_2(dppm)_2(CN)_4$ [dppm = bis(diphenylphosphino)methane]. *Inorg Chem* 28(15):2908–2910.
54. Buss CE, et al. (1998) Structural investigations of vapochromic behavior. X-ray single-crystal and powder diffraction studies of $[Pt(CN\text{-}iso\text{-}C_3H_7)_4][M(CN)_4]$ for M = Pt or Pd. *J Am Chem Soc* 120(31):7783–7790.
55. Hunter BM, et al. (2012) M-M bond-stretching energy landscapes for $M_2(dimen)_4^{2+}$) (M = Rh, Ir; dimen = 1,8-diisocyanomenthane) complexes. *Inorg Chem* 51(12): 6898–6905.
56. Spector MS, Selinger JV, Schnur JM (2003) Chiral molecular self-assembly in Materials—Chirality. *Topics in Stereochemistry (Vol 24)*, Green MM, Meijer EW, Nolte RJM, eds (John Wiley & Sons), pp 281–372.
57. Hill DJ, Mio MJ, Prince RB, Hughes TS, Moore JS (2001) A field guide to foldamers. *Chem Rev* 101(12):3893–4012.
58. Cornelissen JJLM, Rowan AE, Nolte RJM, Sommerdijk NAJM (2001) Chiral architectures from macromolecular building blocks. *Chem Rev* 101(12):4039–4070.
59. Nakano T, Okamoto Y (2001) Synthetic helical polymers: Conformation and function. *Chem Rev* 101(12):4013–4038.
60. Green MM, et al. (2001) Chiral studies across the spectrum of polymer science. *Acc Chem Res* 34(8):672–680.
61. Hirschberg JHK, et al. (2000) Helical self-assembled polymers from cooperative stacking of hydrogen-bonded pairs. *Nature* 407(6801):167–170.
62. Fenniri H, et al. (2001) Helical rosette nanotubes: Design, self-assembly, and characterization. *J Am Chem Soc* 123(16):3854–3855.
63. Percec V, et al. (2004) Self-assembly of amphiphilic dendritic dipeptides into helical pores. *Nature* 430(7001):764–768.
64. Okamoto Y, Yashima E (1998) Polysaccharide derivatives for chromatographic separation of enantiomers. *Angew Chem Int Ed* 37(8):1020–1043.
65. Guo Y-M, Oike H, Saeki N, Aida T (2004) One-pot optical resolution of oligopeptide helices through artificial peptide bundling. *Angew Chem Int Ed Engl* 43(37): 4915–4918.
66. Fenniri H, Deng B-L, Ribbe AE (2002) Helical rosette nanotubes with tunable chiroptical properties. *J Am Chem Soc* 124(37):11064–11072.
67. Nonokawa R, Yashima E (2003) Detection and amplification of a small enantiomeric imbalance in alpha-amino acids by a helical poly(phenylacetylene) with crown ether pendants. *J Am Chem Soc* 125(5):1278–1283.
68. Guo YM, Oike H, Aida T (2004) Chiroptical transcription of helical information through supramolecular harmonization with dynamic helices. *J Am Chem Soc* 126(3): 716–717.
69. Yashima E, Maeda K, Nishimura T (2004) Detection and amplification of chirality by helical polymers. *Chem Eur J* 10(1):42–51.
70. Feringa BL, Delden RA; van Delden RA (1999) Absolute asymmetric synthesis: The origin, control, and amplification of chirality. *Angew Chem Int Ed Engl* 38(23): 3418–3438.
71. Okamoto Y, Nakano T (1994) Asymmetric polymerization. *Chem Rev* 94(2):349–372.
72. Reggelin M, Doerr S, Klussmann M, Schultz M, Holbach M (2004) Helically chiral polymers: A class of ligands for asymmetric catalysis. *Proc Natl Acad Sci USA* 101(15): 5461–5466.
73. Goodby JW (1998) *Handbook of Liquid Crystals: Fundamentals* (Wiley, Weinheim, Germany), pp 115–132.
74. Green MM, et al. (1998) Mechanism of the transformation of a Stiff polymer lyotropic nematic liquid crystal to the cholesteric state by dopant-mediated chiral information transfer. *J Am Chem Soc* 120(38):9810–9817.
75. Oda M, et al. (2000) Circularly polarized electroluminescence from liquid-crystalline chiral polyfluorenes. *Adv Mater* 12(5):362–365.
76. Kauranen M, et al. (1995) Supramolecular second-order nonlinearity of polymers with orientationally correlated chromophores. *Science* 270(5238):966–969.
77. Verbiest T, et al. (1998) Strong enhancement of nonlinear optical properties through supramolecular chirality. *Science* 282(5390):913–915.
78. von Zelewsky A (1999) Stereoselective synthesis of coordination compounds. *Coord Chem Rev* 811:190–192.
79. Barboiu M, Lehn J-M (2002) Dynamic chemical devices: Modulation of contraction/extension molecular motion by coupled-ion binding/pH change-induced structural switching. *Proc Natl Acad Sci USA* 99(8):5201–5206.
80. Berl V, Huc I, Khoury RG, Krische MJ, Lehn J-M (2000) Interconversion of single and double helices formed from synthetic molecular strands. *Nature* 407(6805):720–723.
81. Irie M, Yorozu T, Hayashi K (1987) Steric effect on fluorescence quenching of 1,1′-binaphthyl by chiral amines. *J Am Chem Soc* 100(7):2236–2237.
82. Cram DJ (1992) Molecular container compounds. *Nature* 356(6364):29–36.
83. James TD, Sandanayake KRA, Shinkai S (1995) Chiral discrimination of monosaccharides using a fluorescent molecular sensor. *Nature* 374(6520):345–347.
84. Pu L (2004) Fluorescence of organic molecules in chiral recognition. *Chem Rev* 104(3): 1687–1716.
85. Chen Y, Yekta S, Yudin AK (2003) Modified BINOL ligands in asymmetric catalysis. *Chem Rev* 103(8):3155–3212.
86. Pu L (1998) 1,1′-Binaphthyl dimers, oligomers, and polymers: Molecular recognition, asymmetric catalysis, and new materials. *Chem Rev* 98(7):2405–2494.
87. Lee SJ, Lin W (2008) Chiral metallocycles: Rational synthesis and novel applications. *Acc Chem Res* 41(4):521–537.
88. Bunzen J, Bruhn T, Bringmann G, Lützen A (2009) Synthesis and helicate formation of a new family of BINOL-based bis(bipyridine) ligands. *J Am Chem Soc* 131(10): 3621–3630.
89. Akine S, Nagumo H, Nabeshima T (2012) Hierarchical helix of helix in the crystal: Formation of variable-pitch helical π-stacked array of single-helical dinuclear metal complexes. *Inorg Chem* 51(10):5506–5508.
90. Gin MS, Yokozawa T, Prince RB, Moore JS (1999) Helical bias in solvophobically folded oligo(phenylene ethynylene)s. *J Am Chem Soc* 121(11):2643–2644.
91. Hill DJ, Moore JS (2002) Helicogenicity of solvents in the conformational equilibrium of oligo(*m*-phenylene ethynylene)s: Implications for foldamer research. *Proc Natl Acad Sci USA* 99(8):5053–5057.
92. Gan Q, et al. (2011) Helix-rod host-guest complexes with shuttling rates much faster than disassembly. *Science* 331(6021):1172–1175.
93. Baruah PK, Gonnade R, Rajamohanan PR, Hofmann HJ, Sanjayan GJ (2007) BINOL-based foldamers—access to oligomers with diverse structural architectures. *J Org Chem* 72(14):5077–5084.
94. Frisch MJ, et al. (2010) Gaussian 09 (Gaussian, Inc., Wallingford, CT), Revision C.01.
95. Zhao Y, Truhlar DG (2008) The M06 suite of density functionals for main group thermochemistry, thermochemical kinetics, noncovalent interactions, excited states, and transition elements: Two new functionals and systematic testing of four M06-class functionals and 12 other functionals. *Theor Chem Acc* 120(1-3):215–241.
96. Marenich AV, Cramer CJ, Truhlar DG (2009) Universal solvation model based on solute electron density and on a continuum model of the solvent defined by the bulk dielectric constant and atomic surface tensions. *J Phys Chem B* 113(18):6378–6396.
97. Zhao Y, Truhlar DG (2008) Density functionals with broad applicability in chemistry. *Acc Chem Res* 41(2):157–167.
98. Andrae D, Häussermann U, Dolg M, Stoll H, Preuß H (1990) Energy-adjusted *ab initio* pseudopotentials for the second and third row transition elements. *Theor Chim Acta* 77(2):123–141.
99. Dolg M, Pyykkö P, Runeberg N (1996) Calculated structure and optical properties of $Tl_2Pt(CN)_4$. *Inorg Chem* 35(25):7450–7451.
100. Hehre WJ, Ditchfield R, Pople JA (1972) Self-consistent molecular orbital methods. XII. Further extensions of Gaussian-type basis sets for use in molecular orbital studies of organic molecules. *J Chem Phys* 56(5):2257–2261.
101. Hariharan PC, Pople JA (1973) The influence of polarization functions on molecular orbital hydrogenation energies. *Theor Chim Acta* 28(3):213–222.
102. Francl MM, et al. (1982) Self-consistent molecular orbital methods. XXIII. A polarization-type basis set for second-row elements. *J Chem Phys* 77(7):3654–3665.
103. Dunning TH, Jr. (1989) Gaussian basis sets for use in correlated molecular calculations. I. The atoms boron through neon and hydrogen. *J Chem Phys* 90(2): 1007–1023.